INTERNATIONAL JOURNAL OF SATELLITE COMMUNICATIONS AND NETWORKING
Int. J. Satell. Commun. Network. 2005; **23**:203–228
Published online in Wiley InterScience (www.interscience.wiley.com). DOI: 10.1002/sat.815

Deep-space communications with a 2-hop downlink with high link-availability

Emilio Matricciani*,†

Dipartimento di Elettronica e Informazione, Politecnico di Milano, Piazza L. da Vinci, 32, 20133 Milan, Italy

SUMMARY

We recall and discuss the theory of a 2-hop downlink in deep-space communications. The first hop (length d_1) links the deep-space spacecraft to either a geostationary satellite or to a low Earth orbiting satellite. The second hop (length d_2, with $d_2 \ll d_1$) links the satellite to the Earth receiver through a transparent or regenerative transponder, in slant paths affected by troposphere attenuation. If we adopt a BPSK or QPSK modulation scheme and the same carrier frequencies in the two hops with a transparent transponder, a particular value of the carrier frequency makes the noise-to-signal ratio minimum. A better choice is to assign a low carrier frequency (X-band) to the second hop and a high one (W-band) to the first hop. A 2-hop downlink is superior to a 1-hop downlink with a large power gain proportional to $(d_1/d_2)^2 \gg 1$ at high microwave frequencies and large troposphere attenuation (high link-availability). Shannon's capacity theorem provides the same large gain independently of the choice of the carrier frequencies in the two hops, if we use a regenerative transponder. The carrier frequencies of a 2-hop downlink need not be those reserved to deep-space communication, because the spacecraft could communicate as if it were transmitting 'from the Earth' through a conventional satellite connection. We have applied the theory to a first-order design in the frequency range 10–100 GHz, slant path elevation angles 30°, 45° and 90° at Gera Lario or Fucino (Italy), and downlinks form Mars and Saturn, although the general findings and methodology are of global applicability. Copyright © 2005 John Wiley & Sons, Ltd.

KEY WORDS: satellite communication; deep-space downlink; regenerative transponder; transparent transponder; troposphere attenuation; rain attenuation; Mars; Saturn; Shannon capacity

1. INTRODUCTION

One of the primary goals of NASA's long term plans is to establish a virtual presence throughout the solar system [1], a purpose that can be achieved only if a significant communication capacity can be provided to spacecrafts at very large distances. Using higher frequency bands instead of the current X-band (8.4 GHz) can provide this capacity. The next bandwidth allocated for deep-space communications is at Ka-band (32 GHz). The use of

*Correspondence to: Emilio Matricciani, Dipartimento di Elettronica e Informazione, Politecnico di Milano, Piazza L. da Vinci, 32, 20133 Milan, Italy.
†E-mail: matricci@elet.polimi.it

Ka-band offers a fourfold performance advantage over X-band, because of the f^2-law increase of directivity of the downlink beam as one moves to higher frequencies. This opens up a possible and useful trade space for Ka-band missions with the same antenna size and radio frequency power, since a Ka-band mission can return four times more data than a comparable X-band mission. Each mission will be able to optimize these trades to best benefit from Ka-band's fourfold advantage [2]. Of course, this argument can be extended to higher frequency bands, such as W-band (90 GHz), with obviously larger advantages than those obtainable at Ka-band, once enough power and electrically larger antennas are provided to the spacecraft, as the technology becomes mature.

Whichever is the frequency band, the current design has very often considered a 1-hop communication link, i.e. a '1-shot' communication from the spacecraft (orbiting around a planet or standing on its surface) to the Earth, with physically large receiving antennas, as those of the NASA's Deep Space Network. Only few early studies considered a 2-hop downlink design at microwaves and, more recently, at optical frequencies [3].

The 1-hop design is best suited to X-band downlinks because of the very low impact of the Earth troposphere on the link power budget. But this may not be the case at Ka-band and beyond, because at these frequencies the attenuation of the Earth troposphere can be large, and if we wish to provide a significant capacity in adverse weather conditions during the intervals of spacecraft visibility from the Earth station (contact time), an extra attenuation must be considered, besides that due to free-space.

In our renewed study of a 2-hop downlink (see References [3,4] for earlier studies), the first hop will link the deep-space spacecraft to either a geostationary satellite or to a low Earth orbiting satellite (e.g. a space station); the second hop will link the satellite (or space station) to the final Earth terminal. The satellite transponder can provide only amplification and frequency conversion ('transparent', 'bent-pipe' transponder) or demodulation and bits regeneration (regenerative transponder). In both cases, however, when the performance of the 2-hop downlink is compared to that of the 1-hop downlink, we will show that the advantage of the 2-hop downlink can be very large to allow several trade-offs in a final implementation, and that it can provide a communication capacity with high link-availability, otherwise very difficult or impossible to achieve with a 1-hop downlink. Moreover, the 2-hop downlink is not necessarily constrained to use a carrier frequency in a band assigned to deep-space communication by international regulations, as a 1-hop downlink does. In a 2-hop downlink, in fact, the power received on the Earth can be of the same order of magnitude of the other Earth-based communication links, so that it is not likely to be interfered as, on the contrary, it could happen to the very low power received from deep-space in a 1-hop downlink, if it shared the same frequency bands.

The purpose of the paper is not to design a deep-space downlink to the last detail and consider its overall costs (it is not our expertise), but to assess if our design promises to work well and effectively.

The paper is organized as follows. Section 2 defines the troposphere total attenuation and channel modelling; Section 3 sets the theory of a 2-hop downlink with transparent transponder; Section 4 considers a 1-hop downlink; Sections 5 compares the performance of the two downlinks by defining a useful figure of merit, the gain; Section 6 sets the theory of a 2-hop downlink with regenerative transponder and Section 7 defines a figure of merit for this case, the improvement; Section 8 compares the two downlinks according to Shannon's capacity theorem; Section 9, discusses system architecture; Section 10, as an exercise, applies the theory

to case studies; Section 11 draws some general conclusions. Appendices A and B report useful formulas.

Before proceeding, let us define the following mathematical symbols:

- $A(f,\theta)$, total Earth troposphere attenuation (dB) at carrier frequency f and elevation angle θ;
- A_{r1}, effective area of the receiving antenna onboard the satellite (or space station);
- A_{r2}, effective area of the receiving antenna on the Earth;
- A_{t1}, effective area of the transmitting antenna onboard the deep-space spacecraft;
- A_{t2}, effective area of the transmitting antenna onboard the satellite (or space station);
- $B_e = R/2$, noise bandwidth of the equivalent ideal baseband channel;
- C_{1h}, capacity (bit/s) of an ideal channel according to Shannon, 1-hop downlink;
- C_{2h}, capacity (bit/s) of an ideal channel according to Shannon, 2-hop downlink;
- c, speed of light in free-space propagation;
- d_1, distance between the spacecraft and the satellite (or space station), first hop;
- d_2, distance between the geostationary satellite (or space station) and the Earth receiver, second hop;
- E_{r1}, received energy per bit onboard the satellite;
- E_{r2}, received energy per bit on the Earth;
- f_e, frequency at which $R_{o,1} = R_{o,2}$ (transparent transponder);
- f_1, carrier frequency of the first hop;
- f_2, carrier frequency of the second hop;
- $f_{m,r}$, frequency of minimum noise-to-signal ratio, and probability of bit error, with a regenerative transponder;
- $f_{m,t}$, frequency of minimum probability of bit error with a transparent transponder;
- G, gain of the 2-hop downlink compared to the 1-hop downlink (transparent transponder);
- G_p, power gain of the 2-hop downlink compared to the 1-hop downlink according to Shannon's capacity theorem;
- g_c, forward error correction coding gain in natural units;
- I, improvement of the 2-hop downlink compared to the 1-hop downlink (regenerative transponder);
- $N_{o1} = kT_1$, one-sided power spectrum density (W in 1 Hz bandwidth, k is Boltzman's constant) of the additive white Gaussian noise of the satellite (or space station) receiver;
- $N_{o2} = kT_2$, one-sided power spectrum density (W in 1 Hz bandwidth) of the additive white Gaussian noise of the Earth receiver, considered standing alone, i.e. not connected to the first hop;
- $P_{1h}(e)$, probability of bit error in the 1-hop downlink;
- $P_{2h}(e)$, probability of bit error in the 2-hop downlink;
- $P_1(e)$, probability of bit error in the first hop (regenerative transponder);
- $P_2(e)$, probability of bit error in the second hop (regenerative transponder);
- P_{r1}, received power onboard the satellite (or space station);
- P_{r2}, received power on the Earth;
- P_{t1}, transmitted power from the deep-space spacecraft to the satellite (or to the space station), explicitly termed $P_{t1,1h}$ if its value differs from that of the 2-hop downlink;
- P_{t2}, transmitted power from the Earth orbiting satellite for the signal, i.e., as if it were not connected to the first hop;

- R, total data rate (bit/s), i.e. including coding;
- $R_{o,1h}$, noise-to-signal ratio in the 1-hop downlink, with noise measured in the equivalent noise bandwidth B_e (matched filter);
- $R_{o,2h}$, total noise-to-signal ratio in the 2-hop downlink, with noise measured in the equivalent noise bandwidth B_e (matched filter);
- $R_{o,1}$, noise-to-signal ratio measured in the first hop, with noise measured in the equivalent noise bandwidth B_e (matched filter);
- $R_{o,2}$, noise-to-signal ratio measured in the second hop, with noise measured in the equivalent noise bandwidth B_e (matched filter), considered standing alone, i.e. not connected to the first hop;
- T_1, noise temperature of the Earth orbiting satellite receiver;
- T_2, noise temperature of the Earth receiver.

2. TROPOSPHERE ATTENUATION AND CHANNEL MODELLING

The design of space communication systems working at carrier frequencies above 10 GHz must consider the extra fading due to the troposphere. Rain, snow, water vapour, clouds, oxygen and, to a much less extent, scintillation, can, in fact, seriously degrade a downlink power budget. Some of these attenuations, such as those due to rain and oxygen, depend very much on the carrier frequency.

To present the reader a likely first-order design in the frequency range 10–100 GHz, for slant paths with elevation angles of 30°, 45° and 90° (zenith), we have considered the troposphere total attenuation that can be measured at Gera Lario (46.2° N, 9.4° E, 210 m above mean sea level, Northern Italy), a locality with weather conditions quite severe, and Fucino (42.0° N, 13.6° E, 680 m, Central Italy), with weather conditions less severe (in both sites there is a Telespazio space station), although the general findings and methodology are of global applicability. A geostationary satellite located at the same longitude of the Earth receiving station is seen with an elevation angle of about 37° at Gera Lario and 41° at Fucino.

The rain attenuation, A_R (dB), exceeded in an average year for a fraction of time at a carrier frequency f at the two sites has been estimated by a reliable empirical formula [5] (see also Appendix A). The formula links A_R to f, and to the slant path elevation angle, for a fixed fraction of time, for instance 0.01% (availability 99.99% of the time), an outage percentage that can correspond to high troposphere attenuation. The extra fading due to water vapour, clouds, oxygen and scintillations for the same fraction of time have been estimated and combined together with A_R according to the ITU-R [6–8], formulas not reported for brevity.

Figure 1 shows the troposphere total attenuation, $A(f, \theta)$ (dB), at the two sites, as a function of carrier frequency f , exceeded for a fraction of time equal to 0.01%, in a slant path with elevation angle $\theta = 30°$. Figure 2 shows how $A(f, \theta)$ changes as a function of elevation angle, at Gera Lario. As the elevation angle increases, up to the local zenith, the total attenuation largely decreases because of the 'secant law' (see Appendix A). In any case, in the interval 55–65 GHz no communication with the Earth is possible because of the extreme attenuation due to oxygen. Notice that if we exclude this interval, rain is the largest source of extra attenuation.

Since $A(f, \theta)$ is not frequency selective, even for relatively large bandwidths to be used in practical systems, and no shadowing, blockage or delayed rays (multipath) will be present in well located and designed fixed earth terminals, and scattering due to rain is still negligible, the overall channel is affected only by an in-band 'flat' attenuation and additive white Gaussian

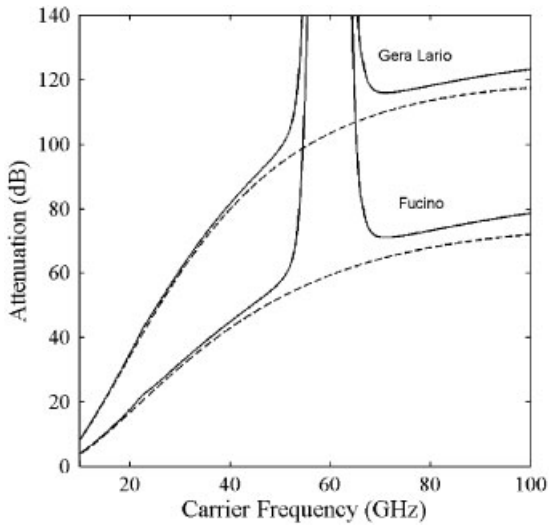

Figure 1. Troposphere total attenuation, $A(f)$ (dB) as a function of carrier frequency f, in the frequency range 10–100 GHz, exceeded for a fraction of time 0.01%, in a slant path with elevation angle $\theta = 30^{\circ}$. Dashed lines refer to rain attenuation only; Equation (A1) scaled according to (A2), see also Reference [5]. The extra fading due to water vapour, clouds, oxygen and scintillations have been estimated and combined together with rain attenuation according to the ITU-R [6–8].

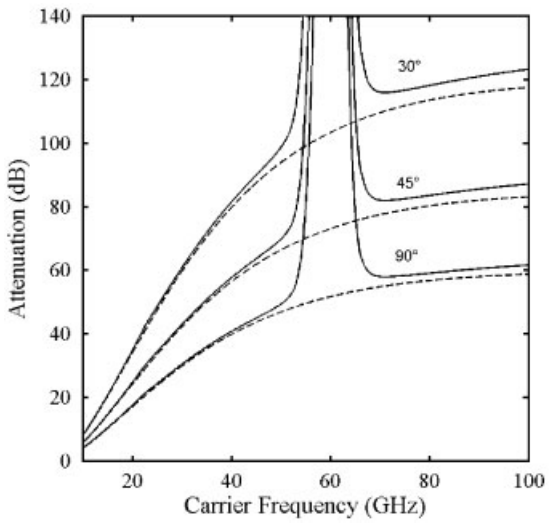

Figure 2. Troposphere total attenuation, $A(f)$ (dB), at Gera Lario as a function of carrier frequency f, in the frequency range 10–100 GHz, exceeded for a fraction of time 0.01%, in a slant path with elevation angle $\theta = 30^{\circ}$, $\theta = 45^{\circ}$, $\theta = 90^{\circ}$. Dashed lines refer to rain attenuation only; Equation (A1) scaled according to Equation (A2), see also Reference [5]. The extra fading due to water vapour, clouds, oxygen and scintillations have been estimated and combined together with rain attenuation according to the ITU-R [6–8].

noise. Moreover, the transfer medium is substantially made up of free-space propagation in the first hop (spacecraft-to-satellite), and free-space propagation and additive (in dB) 'flat' attenuation in the second hop (satellite-to-Earth), so that the equivalent baseband channel is ideal, Gaussian, and measures the same total flat attenuation and noise of the radio frequency channel.

As we are interested in showing first-order values of the parameters, we do not consider further losses (e.g. antenna pointing and polarization mismatch), or intersymbol interference.

In other words, for our study, we can use the equivalent baseband channel of BPSK or QPSK (modulation schemes used in deep-space communication): it is an ideal low pass Gaussian channel which can deliver the same bit rate R with the same probability of bit error $P(e)$, with half the bandwidth of that allocated at radio frequency for BPSK, or with the same bandwidth for QPSK, and with the same total carrier power and affected by the same radio frequency additive white Gaussian noise (see Reference [5, Figure 11]).

The results below, however, can be applied to other modulation schemes, with the same general conclusions, as Shannon's capacity theorem shows (see Section 8).

Now, let us first study the case of a 2-hop downlink with a transparent transponder.

3. 2-HOP DOWNLINK WITH TRANSPARENT TRANSPONDER

Let us first calculate the noise-to-signal energy and power ratio we can obtain in a 2-hop downlink with a transparent transponder onboard the satellite (or space station), with matched receivers with a BPSK or QPSK modulation. Next, we will consider two cases: (a) same carrier frequencies, and (b) different carrier frequencies for the two hops.

3.1. Noise-to-signal power ratio

We use the less common noise-to-signal (or carrier) energy and power ratio (a use that goes back to Panter [9]), instead of the signal-to-noise ratio, because, in our opinion, it provides more insight for studying and designing a multi-hop communication system.

Since the additive white Gaussian noise sources of the two hops are statistically independent, standard calculations yield the following noise-to-signal ratio of the 2-hop downlink (see Appendix B):

$$R_{\mathrm{o,2h}} = R_{\mathrm{o,1}} + R_{\mathrm{o,2}} = \frac{N_{\mathrm{o1}}/2}{E_{\mathrm{r1}}} + \frac{N_{\mathrm{o2}}/2}{E_{\mathrm{r2}}} = \frac{N_{\mathrm{o1}} B_{\mathrm{e}}}{P_{\mathrm{r1}}} + \frac{N_{\mathrm{o2}} B_{\mathrm{e}}}{P_{\mathrm{r2}}} \tag{1}$$

In Equation (1) $P_{\mathrm{r}} = E_{\mathrm{r}} R$ is the received average power per bit. Now, let us include in Equation (1) free-space propagation, troposphere total attenuation (in the following, we neglect possible fading due to the atmosphere of other planets, such as Mars) and the coding gain g_{c} of a forward error correcting code. We get

$$R_{\mathrm{o,2h}} = \frac{N_{\mathrm{o1}} B_{\mathrm{e}} c^2}{P_{\mathrm{t1}} A_{\mathrm{t1}} A_{\mathrm{r1}} g_{\mathrm{c}}} \left(\frac{d_1}{f_1}\right)^2 + \frac{N_{\mathrm{o2}} B_{\mathrm{e}} c^2}{P_{\mathrm{t2}} A_{\mathrm{t2}} A_{\mathrm{r2}} g_{\mathrm{c}}} \left(\frac{d_2}{f_2}\right)^2 \times 10^{A(f_2,\theta)/10} \tag{2}$$

In Equation (2) we keep explicit the effective areas of the antennas (the effective area A is a function of the geometrical area A_g through the efficiency, assumed to be 0.6 for all antennas, i.e. $A = 0.6A_g$) rather than their gains, because their physical size and weight are important constraints onboard the satellite and deep-space spacecraft.

Standard calculations show that the probability of bit error in the 2-hop radio link is given by the $Q(x)$ function

$$P_{2h}(e) = Q(x) = \int_x^{+\infty} \frac{1}{\sqrt{2\pi}} e^{-y^2/2}\, dy$$

$$\cong \frac{1}{\sqrt{2\pi x}} e^{-x^2/2} \quad \text{for } Q(x) < 10^{-2} \tag{3}$$

in which

$$x^2 = \frac{1}{R_{o,2h}} \tag{4}$$

Let us study expression (2). Of the many variables we choose to keep transmitters' power and antennas' effective area constant because of the likely trade-offs (mentioned in Section 1) that could be considered for a particular mission, and study the impact of the carrier frequency (i.e. frequency band) on the overall noise-to-signal power ratio. We will study transmitters' power trade-offs in Section 8 according to Shannon's capacity theorem.

3.2. *Design with the same carrier frequencies* ($f_2 = f_1$)

An obvious technological and economical choice is to set $f_1 = f_2 = f$, and consider f an independent variable to be fixed according to some best choice. Of course, the two specific carrier frequencies must not overlap their modulated spectra, otherwise on-board the satellite the transmitted beam to the Earth would interfere with the received beam from the deep-space spacecraft. Notice, however, that the small difference between f_1 and f_2 to be considered in a real design would not affect the results below.

Now, if both hops use the same carrier frequency, we realize that Equation (2) can have a *minimum* value, and thus yield also a minimum probability of bit error, according to (3) and (4), at a carrier frequency $f_{m,t}$ that, for a given site and total attenuation (or fraction of time) considered, can fall in a useful microwave range. In fact $A(f, \theta)$, which is expressed in dB, is a fast increasing function of frequency (see Figures 1 and 2), mainly because of rain attenuation and oxygen, so that the exponential term in Equation (2) can increase very much with frequency, and can make the second addend equal or even larger that the first one, even if $d_2 \ll d_1$ (as it is the case), as if there were an effective distance, d_e, equal to

$$d_e = d_2 \times 10^{A(f,\theta)/20} \tag{5}$$

By adding $20 \log_{10} d_2$ to $A(f, \theta)$ shown in Figures 1 and 2 we can also draw d_e as a function of frequency.

Let us study the behaviour of Equation (2) at high ($\sim$ 100 GHz) and low ($\sim$ 10 GHz, or X-band) frequencies, which translate into high and low attenuation, respectively. At high

frequencies we get the following expression:

$$R_{o,2h}(f,\theta) \approx R_{o2} = \frac{N_{o2}B_e c^2 d_2^2}{P_{t2}A_{t2}A_{r2}g_c} \times \frac{10^{A(f,\theta)/10}}{f^2}$$
$$= \frac{N_{o2}B_e c^2}{P_{t2}A_{t2}A_{r2}g_c} \times \frac{d_e^2}{f^2} \quad \text{for high } f \tag{6}$$

This expression is very likely an increasing function of frequency because of $10^{A(f,\theta)/10}$ (to be verified for the particular site and probability), and is only due to the second hop which, as a consequence, fixes the overall noise-to-signal power ratio and $P(e)$, calculated by (3), with (4) given by the limit (6). In this case we surely find $d_e \gg d_1$, and the downlink is dominated by the second hop.

For lower frequencies, such as X-Band, $A(f,\theta)$ is negligible (the 2-hop design is less effective) and we get only the first addend

$$R_{o,2h} \cong R_{o1} = \frac{N_{o1}B_e c^2 d_1^2}{P_{t1}A_{t1}A_{r1}g_c} \times \frac{1}{f^2} \quad \text{for small } f \tag{7}$$

so that $d_1 \gg d_e$, and the first hop determines the overall noise-to-signal power ratio and $P(e)$, calculated by (3), with (4) given by the limit (7). As a consequence of the above analysis, as anticipated, a *minimum* can exist at a certain frequency $f_{m,t}$.

The minimum can be found by standard calculus (frequency derivative of Equation (2) set to zero, Appendix B) but it can be shown (see Section 10 for a graphical example) that $f_{m,t}$ is less than (and of the same order of magnitude of) the frequency f_e for which $R_{o,1} = R_{o,2}$, i.e. the frequency at which $R_{o,2h}$ is 3 dB larger than either one of the two addends in Equation (2). By imposing $R_{o,1} = R_{o,2}$, it turns out that f_e is the frequency that makes the equivalent distance equal to

$$d_e(f_e,\theta) = d_2 \times 10^{A(f_e,\theta)/20} = \sqrt{\frac{T_1}{T_2}}\sqrt{\frac{P_{t2}A_{t2}A_{r2}}{P_{t1}A_{t1}A_{r1}}} \times d_1$$
$$\cong \sqrt{\frac{T_1}{T_2}} \times d_1 \quad \text{for } P_{t2}A_{t2}A_{r2} \cong P_{t1}A_{t1}A_{r1} \tag{8}$$

By (numerically) solving Equation (8) we can get f_e.

3.3. *Design with different carrier frequencies* ($f_2 \neq f_1$)

Up to now we have always considered the same frequency band for both hops. We can use, however, two different carrier frequencies. The best choice is to assign the lower frequency to the second hop to measure smaller troposphere attenuation, and the higher one to the first hop to take advantage of the higher gains that can be obtained with antennas of fixed size at high microwave frequencies, such as W-band (90 GHz).

In this case the short satellite–Earth link could be designed at X-band (with negligible or small troposphere attenuation) or at Ka-band (e.g. $f_2 = 32$ GHz to comply with international frequency assignments, although this is not strictly necessary for a 2-hop downlink as mentioned in Section 1), and the long spacecraft-satellite link could be designed at a higher carrier frequency, e.g. 90 GHz, to profit from the large antennas gain obtainable with physically small parabolic antennas, or the like, once the technology for this band is mature. The first hop will not be interfered from Earth transmitters working in the same band because of the large oxygen

attenuation. Of course, a design with $f_2 \ll f_1$ is more suited because it can 'match' radio electrical parameters (frequencies, antenna gains, transmitters' power, troposphere attenuation) more closely to the two largely different hops.

If f_1 is a constant and we let $f_2 = f$ be a design parameter, then Equation (2) is very likely to be an increasing function of frequency, the performance of which is determined by the first hop at the lower frequencies, and by the second hop at the higher frequencies.

4. 1-HOP DOWNLINK

If we implement a 1-hop downlink with the same parameters of the 2-hop downlink onboard the deep-space spacecraft and on the Earth, we obtain the following noise-to-signal ratio:

$$R_{o,1h} = \frac{N_{o2} B_e c^2}{P_{t1} A_{t1} A_{r2} g_c} \left(\frac{d_1 + d_2}{f} \right)^2 \times 10^{A(f,\theta)/10} \tag{9}$$

Notice that the exact combination of d_1 and d_2 in Equation (9) is not important because $d_2 \ll d_1$.

Now $P_{1,h}(e)$ is given by Equation (3) with

$$x^2 = \frac{1}{R_{o,1h}} \tag{10}$$

In the range of frequency considered, Equation (9) is very likely an increasing function of frequency so that, as in the case $f_1 =$ constant discussed in Section 3.3, the minimum noise-to-signal ratio should be at the lowest frequency considered. Of course, in this case the 'match' discussed in Section 3 is not possible.

5. GAIN

We wish to compare the 2-hop downlink performance with transparent transponder with that of the 1-hop downlink, and to assess when the 2-hop downlink performs better than the 1-hop downlink, by keeping constant all other parameters listed in Section 1 but the carrier frequency. As a figure of merit of this comparison, independent of g_c and B_e, we assume the ratio, termed *gain*, between the noise-to-signal ratios in the two downlinks:

$$G = \frac{R_{o,1h}}{R_{o,2h}} \tag{11}$$

The 2-hop downlink will perform better if $G > 1$, i.e. if $R_{o,1h} > R_{o,2h}$. Since $P(e)$ is given by Equation (3) with the noise-to-signal ratios of Equation (11), it follows from Equation (3) that $P_{1h}(e) \gg P_{2h}(e)$ when $R_{o,1h} > R_{o,2h}$ for only few decibels.

First, let us assume the case $f_2 = f_1 = f$. Using the approximate expression for $Q(x)$, Equation (3), standard calculations show that when f is large and $A(f, \theta)$ gets large too, G exhibits

a horizontal asymptote given by

$$G_{\text{high}} = \frac{P_{t2}A_{t2}}{P_{t1}A_{t1}}\left(\frac{d_1 + d_2}{d_2}\right)^2$$
$$G_{\text{high}} \cong \left(\frac{d_1}{d_2}\right)^2 \quad \text{for } P_{t1}A_{t1} \cong P_{t2}A_{t2} \text{ and } d_2 \ll d_1 \tag{12a}$$

Before applying (12a), the value of $P(e)$ obtainable from (2) and (3) must always be checked to assess if it is smaller than 10^{-2}, to apply (3), and below the maximum value tolerated by the user, to be useful.

Because of (12a), G (in dB) can be of the order of the total troposphere attenuation (Figures 1 and 2) when $f_2 = f_1$. In fact, if we consider a design at the frequency of minimum, approximately given by f_e (Section 3.2), it is very likely that the gain obtainable at this frequency is close to G_{high} (e.g. see Figures 4 and 6). If this applies then from Equations (12a) and (8) we get

$$G_{\text{high}} \cong \left(\frac{d_1}{d_2}\right)^2 = \left(\frac{d_2 \times 10^{A(f_e,\theta)/20}}{d_2}\sqrt{\frac{T_2}{T_1}}\right)^2 = 10^{A(f_e,\theta)/10} \times \frac{T_2}{T_1} \tag{12b}$$

so that $G_{\text{high}}(\text{dB}) \cong A(\text{dB})$ for $T_2 \cong T_1$. It is mainly this factor that can make the 2-hop downlink design in principle more effective than the 1-hop downlink design.

When f is low (e.g. X-band), $A(f, \theta) \cong 0$ dB. Now, since $d_2 \ll d_1$ G approaches the limit

$$G_{\text{low}} \cong \left(\frac{T_2}{T_1}\right)\left(\frac{A_{r1}}{A_{r2}}\right) \tag{13a}$$

Equation (13a) states that, even at X-band, the gain of a 2-hop downlink can be significant and useful if the value of $P(e)$ obtainable is tolerable.

Let us now assume $f_2 \neq f_1$. Because, as discussed previously, the best choice would be to adopt $f_2 \ll f_1$, e.g. $f_1 = 90$ GHz, let us first consider this case. As $A(f, \theta) \cong 0$ dB and $d_2 \ll d_1$, the gain approaches the limit

$$G_{\text{low}} \cong \left(\frac{T_2}{T_1}\right)\left(\frac{A_{r1}}{A_{r2}}\right)\left(\frac{f_1}{f_2}\right)^2 \tag{13b}$$

We find the f^2-law increase mentioned in Section 1, but also a dependence on the ratios of receivers' noise temperatures and effective areas of the receiving antennas, so that the gain can be significant even at X-band and larger than that given by Equation (13a), confirming that the design with $f_2 \ll f_1$ is better than the design with $f_2 = f_1$.

At high frequencies, i.e. when $f_2 \to f_1$, it can be shown that G_{high} is, of course, given by Equation (12a), as for the case $f_2 = f_1$.

Table I summarizes the formulas found for these limits. According to Table I, the design with $f_2 \neq f_1$ is always better than the design with $f_2 = f_1$ and they coincide when $f_2 \to f_1$.

6. 2-HOP DOWNLINK WITH REGENERATIVE TRANSPONDER

Let us examine the case of a regenerative transponder on board the satellite, and compare its $P(e)$ with that obtainable in the 1-hop downlink, the latter given by (9), (10) and (3). In this case the probability of bit error in the 2-hop downlink, for statistically independent errors and small

Table I. Limits of the gain G for high and low frequencies in a 2-hop downlink with transparent transponder, for $d_2 \ll d_1$, for BPSK and QPSK modulation schemes.

Frequency of 1st and 2nd hop	G_{low}	G_{high}
$f_2 = f_1 = f$	$\left(\frac{T_2}{T_1}\right)\left(\frac{A_{\text{r1}}}{A_{\text{r}_2}}\right)$	$\frac{P_{\text{t2}}A_{\text{t2}}}{P_{\text{t1}}A_{\text{t1}}}\left(\frac{d_1}{d_2}\right)^2$
$f_2 = f < f_1$	$\left(\frac{T_2}{T_1}\right)\left(\frac{A_{\text{r1}}}{A_{\text{r}_2}}\right)\left(\frac{f_1}{f_2}\right)^2$	$\frac{P_{\text{t2}}A_{\text{t2}}}{P_{\text{t1}}A_{\text{t1}}}\left(\frac{d_1}{d_2}\right)^2$
(f_1 = constant)		

At low frequencies (~ 10 GHz) we assume $A(f,\theta) \cong 0$ dB. At high frequencies (~ 100 GHz) we assume a large $A(f,\theta)$ (corresponding to high link-availability). Note that the square root of these formulas provides the limits of the improvement I (Section 7) in a 2-hop downlink with regenerative transponder, i.e. $I_{\text{low}} = \sqrt{G_{\text{low}}}$, $I_{\text{high}} = \sqrt{G_{\text{high}}}$.

probabilities, is given by

$$P_{2\text{h}}(e) = P_1(e) + P_2(e) - P_1(e)P_2(e) \cong P_1(e) + P_2(e) \tag{14}$$

with

$$\begin{aligned} P_1(e) &= Q(x_1) \\ x_1^2 &= \frac{1}{R_{\text{o1}}} \end{aligned} \tag{15a}$$

and

$$\begin{aligned} P_2(e) &= Q(x_2) \\ x_2^2 &= \frac{1}{R_{\text{o2}}} \end{aligned} \tag{15b}$$

The limiting trends are the following. For high frequencies and high attenuation we may get

$$P_{2\text{h}}(e) \cong P_2(e) \tag{16a}$$

so that the second hop determines (dominates) the downlink performance. For low frequencies and low attenuation, we may get

$$P_{2\text{h}}(e) \approx P_1(e) \tag{16b}$$

so that the first hop determines the downlink performance. Again, a minimum can exist at a certain frequency $f_{\text{m,r}}$.

The minimum can be found by standard calculus, but it can be shown (see Section 10 for a graphical example) that $f_{\text{m,r}}$ is less than (and of the same order of magnitude of) the frequency for which $P_1(e) = P_2(e)$, i.e. the frequency at which $P_{2\text{h}}(e)$ is twice larger than either one of the two addends in (14). By imposing this equality, it turns out that this frequency is again f_{e}, Equation (5). Since $f_{\text{m,r}}$ and f_{e} are much closer than $f_{\text{m,t}}$ and f_{e} are for a transparent transponder

(see Section 10 for a graphical example), we can assume

$$f_{m,r} \approx f_e \tag{17}$$

Since a regenerative transponder is more efficient than a transparent one, this minimum will yield a lower $P(e)$ of the corresponding transparent transponder case.

7. IMPROVEMENT

Now, for a regenerative transponder, we wish to compare the 2-hop downlink performance to that of the 1-hop downlink, and to assess when the 2-hop downlink performs better than the 1-hop downlink. As a figure of merit of this comparison we assume the ratio between the probabilities of bit error obtainable in the two downlinks, termed *improvement*, given by

$$I = \frac{P_{1h}(e)}{P_{2h}(e)} = \frac{P_{1h}(e)}{P_1(e) + P_2(e)} \tag{18a}$$

The improvement I is not independent of the gain. By recalling Equations (11), (14), (3), (1) we can write

$$I = \sqrt{G}\,\frac{\sqrt{(R_{o1} + R_{o2})e^{-1/R_{o1h}}}}{\sqrt{R_{o1}e^{-1/R_{o1}}} + \sqrt{R_{o2}e^{-1/R_{o2}}}} \tag{18b}$$

The 2-hop downlink will perform better if $I > 1$, i.e. if $P_{1h}(e) > P_{2h}(e)$.

In the limit cases of low frequency ($A(f,\theta) \cong 0$ dB), and high frequencies (large $A(f,\theta)$, high link-availability) there is no distinction between the performance of a downlink with a transparent transponder and that with a regenerative transponder, so that a regenerative transponder is wasted. In fact, in these limit cases the performance of a downlink with a transparent transponder is dominated only by one hop: the 1st one at low frequencies, the 2nd one at high frequencies, as in the regenerative case, so that the two downlinks are indistinguishable at the Earth receiver because the noise-to-signal ratio and probability of bit error are the same. In these cases, it can be shown from Equation (18b) that, if $d_2 \ll d_1$, the improvement approaches the limits given by

$$I = \sqrt{G} \tag{19}$$

where G is given by Table I, for each combination of carrier frequencies discussed in Section 5. In conclusion, in the limit ranges we can adopt only a single figure of merit, the gain G, for any type of transponder.

The results derived in Sections 7 and 5 are, however, rather general and independent of the modulation and coding schemes adopted, as next section shows.

8. 2-HOP DOWNLINK VERSUS 1-HOP DOWNLINK ACCORDING TO SHANNON

In this section we compare the performance of a 2-hop downlink with that of a 1-hop downlink, by requiring that the capacity C (bit/s), given by Shannon's famous formula, is the same for both downlinks (with a negligible probability of bit error in any hop considered). Then we will

find how the power transmitted by the spacecraft in the 1-hop downlink, $P_{t,1h}$, is related to the power transmitted by the spacecraft or by the satellite, in the 2-hop downlink, P_{t1} or P_{t2}, respectively.

For a *transparent* transponder, by making equal the two channel capacities, we get

$$C_{2h} = B\log_2\left(1+\frac{1}{R_{o,2h}}\right) = C_{1h} = B\log_2\left(1+\frac{1}{R_{o,1h}}\right) \tag{20a}$$

B is a reference bandwidth and $R_{o,2h}$, $R_{o,1h}$ are given by Equations (1), (2) and (9) with B instead of B_e, the value of which, however, does not affect the results below. From Equation (20a), we get

$$R_{o1} + R_{o2} = R_{o,1h} \tag{20b}$$

In terms of the gain G (Section 5) Equation (20b) sets $G = 1$ (0 dB).

Let us assume $f_2 = f_1$ and find how $P_{t,1h}$ is related to either P_{t1} or P_{t2}. By recalling Equations (1), (2), (9) and that $d_2 \ll d_1$, and by solving Equation (20b) for $P_{t,1h}$, we get

$$\frac{1}{P_{t1,1h}} = \frac{T_1}{T_2}\frac{A_{r2}}{P_{t1}A_{r1}\times 10^{A(f,\theta)/10}} + \left(\frac{d_2}{d_1}\right)^2\frac{A_{t1}}{P_{t2}A_{t2}} \tag{21}$$

Now, when the high and low frequencies of Sections 5 and 7 are considered, from Equation (21) we get

$$P_{t1,1h} = G_{p2}P_{t2} = \left(\frac{A_{t2}}{A_{t1}}\right)\left(\frac{d_1}{d_2}\right)^2 P_{t2} \quad \text{high frequencies} \tag{22a}$$

$$P_{t1,1h} = G_{p1}P_{t1} = \left(\frac{A_{r1}}{A_{r2}}\right)\left(\frac{T_2}{T_1}\right)P_{t1} \quad \text{low frequencies} \tag{22b}$$

G_p is the factor (or power gain for a 2-hop downlink) by which the power of either the 1st hop or the 2nd hop must be multiplied to get the power $P_{t,1h}$ necessary in the 1-hop downlink to provide the same performance of the 2-hop downlink.

Since the left-hand member of Equation (20b) is coincident with Equation (2), it follows that C_{2h} is maximum when $f_1 = f_2 = f_{m,t}$, so that Appendix B gives the values of frequencies of maximum capacity.

If $f_2 \neq f_1$ (f_2 is always the carrier frequency assigned both to the 2nd hop of the 2-hop downlink and to the 1-hop downlink), from (20b) we get the limits

$$P_{t1,1h} = G_{p2}P_{t2} = \left(\frac{A_{t2}}{A_{t1}}\right)\left(\frac{d_1}{d_2}\right)^2 P_{t2} \quad \text{high frequencies} \tag{23a}$$

$$P_{t1,1h} = G_{p1}P_{t1} = \left(\frac{T_2}{T_1}\right)\left(\frac{A_{r1}}{A_{r2}}\right)\left(\frac{f_1}{f_2}\right)^2 P_{t1} \quad \text{low frequencies} \tag{23b}$$

Notice that $P_{t1,1h}$ is written as a function of the power transmitted in the most critical hop of the 2-hop downlink, that is the 2nd hop at high frequencies, Equations (22a), (23a), and the 1st hop at low frequencies, Equations (22b), (23a).

Table II. Power gain $G_p = P_{t1,1h}/P_{t1}$, or $G_p = P_{t1,1h}/P_{t2}$ theoretically obtainable in the 2-hop downlink, compared to the 1-hop downlink, for the same performance, according to Shannon's capacity theorem (Section 8), with a transparent transponder. For a regenerative transponder G_p is given by Equation (25), i.e. by the value of the high frequency column below.

Frequency of 1st and 2nd hop	P_{t1} (Low frequency)	P_{t2} (High frequency)
$f_2 = f_1 = f$	$\left(\frac{T_2}{T_1}\right)\left(\frac{A_{r1}}{A_{r_2}}\right)$	$\frac{A_{t2}}{A_{t1}}\left(\frac{d_1}{d_2}\right)^2$
$f_2 = f < f_1$ (f_1 = constant)	$\left(\frac{T_2}{T_1}\right)\left(\frac{A_{r1}}{A_{r_2}}\right)\left(\frac{f_1}{f_2}\right)^2$	$\frac{A_{t2}}{A_{t1}}\left(\frac{d_1}{d_2}\right)^2$

For a *regenerative* transponder, since each hop must provide the same capacity (with negligible probability of bit error), we get

$$B\log_2\left(1+\frac{1}{R_{o1}}\right) = B\log_2\left(1+\frac{1}{R_{o2}}\right) = B\log_2\left(1+\frac{1}{R_{o,1h}}\right) \tag{24a}$$

It follows that

$$R_{o1} = R_{o2} = R_{o,1h} \tag{24b}$$

Since R_{o2} and $R_{o,1h}$ in the range of frequency considered are very likely to be an increasing function of frequency, the maximum capacity should be at the lowest frequency considered.

Now, from Equations (24b), (1), (8), (9), (10b), standard calculations show that $P_{t1,1h}$, regardless of the choice $f_2 = f_1$ or $f_2 \neq f_1$, and for any carrier frequency, is always given by

$$P_{t1,1h} = G_{p2}P_{t2} = \left(\frac{A_{t2}}{A_{t1}}\right)\left(\frac{d_1}{d_2}\right)^2 P_{t2} \tag{25}$$

Equation (25) is the best we can obtain, since the use of a regenerative transponder minimizes the power, compared to a transparent transponder, for the same probability of bit error.

Table II summarizes the results. This table is fundamental because it provides, according to Shannon's capacity theorem, the power gain G_p theoretically obtainable in the 2-hop downlink, compared to the 1-hop downlink, for the same probability of bit error.

9. SYSTEM ARCHITECTURE

When the architecture of the 1-hop downlink currently used is compared to the architecture envisaged for a 2-hop downlink, the differences are many.

A 1-hop downlink implies the use of several very large and dedicated ground stations coordinated to track the very low power coming from the deep-space spacecraft, e.g. with the Deep-Space Network (antenna diameter sizes of 70, 34 and 26 m; the 34-m antenna is being adapted to work at 32 GHz), and requires carrier frequencies reserved only to this service, not to be interfered by conventional satellite and terrestrial links. The Deep-Space Network is deployed at three sites spaced longitudinally about equally around the globe so that deep-space

spacecrafts are always in view of at least one site, if the Earth is visible. During each station contact time, the elevation angle of the 1-hop downlink varies with time so that the noise-to-signal ratio varies also with time because, even in static weather conditions, the fading due to the troposphere increases, on the average, as the elevation angle decreases. As a consequence a largely variable data return is expected (e.g. see Reference [10]).

A 2-hop downlink may need to deploy only one satellite in the geostationary orbit (or maybe more satellites or space stations in lower orbits) and a small earth station, or two small stations connected in a site-diversity configuration to better counteract high rain attenuation. The satellite could be in orbit for other services and could be used, with independent transponders, to track the deep-space spacecraft. One such system could be similar to the Tracking and Data Relay Satellite System.

With this architecture the deep-space spacecraft is always connected to the Earth receiver because the contact time is, theoretically, 24 h, if the Earth is visible. As a consequence, there would be a fixed slant path (with an elevation angle high enough to reduce atmosphere attenuation), and the noise-to-signal ratio and data return would change only because of troposphere attenuation which, however, could be overcome to provide a final constant data rate. Hence, the deep-space spacecraft would communicate as if it were transmitting 'from the Earth' through a conventional 2-hop satellite connection, and, for this reason, the Earth receiver could be placed anywhere in the area covered by the satellite and can be of small size.

A 2-hop downlink is not necessarily constrained to use a carrier frequency assigned to deep-space communication by international regulations, as a 1-hop downlink does, because in the 2-hop downlink the power received on the Earth can be of the same order of magnitude of the other Earth-based communication links so that, if properly designed, it is not likely to be interfered as, on the contrary, it could happen to a 1-hop downlink if it shared the same frequency bands.

10. CASE STUDIES

As an exercise and application of the theory, we adopt a BPSK or QPSK modulation scheme and consider a first-order design of two deep-space downlinks: (a) from the planet Mars ($d_1 \approx 2 \times 10^{11}$ m, i.e. 200 million km); and (b) from the planet Saturn ($d_1 \approx 1.4 \times 10^{12}$ m, i.e. 1400 million km), to a (geostationary) satellite ($d_2 \approx 4 \times 10^7$ m, i.e. 40 000 km) seen at Gera Lario or Fucino.

10.1. Choice of parameters

Let us first fix reasonable and conservative values of the two noise sources. As for the value of T_2, we can assume an antenna noise temperature $T_o = 290$ K because of the troposphere attenuation, mainly due to rain in the useful frequency windows found below. Rain, in fact, can be considered, conservatively, as a dissipative medium at temperature T_o: when its attenuation gets large and is totally attributed to absorption phenomena, the noise temperature at the antenna output is approximately T_o, regardless of the space noise. We assume this conservative design even for low attenuation. Moreover, we assume that the noise added by the receiver is of the order of 50 K [11], so that $T_2 = 340$ K, a pessimistic and conservative value, and that it is

independent of elevation angle. As for T_1 let us assume a satellite (or space station) antenna noise temperature of 30 K and a receiver noise temperature of 50 K [11], i.e. $T_1 = 80$ K.

To present a straight design, we assume a 'reference' deep-space spacecraft with $P_{t1} = P_{t2} =$ 35 W (furnished, at 32 GHz, by a traveling-wave tube amplifier [11]) and 4 identical transmitting and receiving antennas with geometrical diameters of 2.5 m [1] for the Mars downlink (i.e. $A_{t1} = A_{r1} = A_{t2} = A_{r2}$), and $P_{t1} = 100$ W (e.g. Voyager missions [12]) and 4 identical transmitting and receiving antennas with geometrical diameters of 4.0 m (e.g. Cassini spacecraft's high gain antenna [13]) for the Saturn downlink, all with efficiency 0.6, independently of frequency. Remember that we always suppose perfect antennas pointing for a full effective area and gain.

Notice that the choice above reduces the number of parameters and that the design does not require the large receiving antennas of the Deep-Space Network (34-m and 70-m parabolic antennas), which do not easily achieve high efficiency in frequency bands quite higher than X-band.

In all cases we assume a reference $R = 100$ kbit/s coded transmission (e.g. Cassini spacecraft [13]) and a coding gain of 10 dB ($g_c = 10$), provided by one of the latest turbo codes for $P(e) \leqslant 10^{-5}$ [14] (see also Reference [15, Figure 10.27, p. 677]), so that, since we have always applied a constant coding gain, the results for $10^{-5} < P(e) \leqslant 10^{-2}$ are optimistic.

10.2. Mars–Earth downlink

Let us first consider the case of a *transparent* transponder, $f_2 = f_1$, and apply Equations (2) and (3). Figure 3 shows the probability of bit error obtainable at Gera Lario as a function of frequency and elevation angle. The results clearly show minima values, predicted by (2) if $f_2 = f_1$

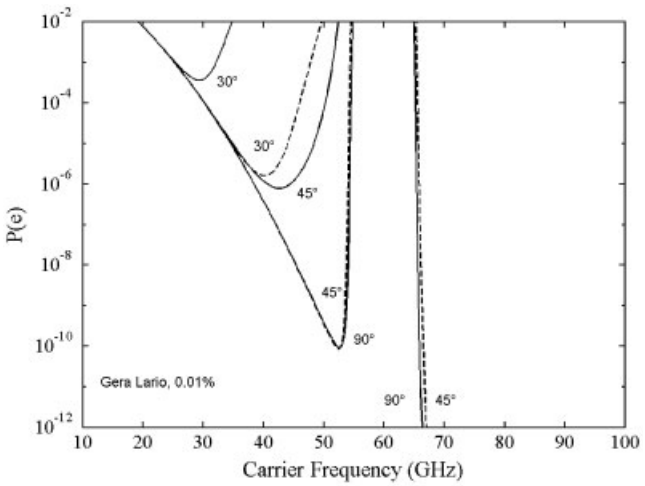

Figure 3. Probability of bit error as a function of carrier frequency ($f_2 = f_1$) and elevation angle, in the frequency range 10–100 GHz, Gera Lario, fraction of time 0.01%. Mars–Earth 2-hop downlink with a transparent transponder onboard a (geostationary) satellite, with $P_{t1} = P_{t2} = 35$ W, 4 identical 2.5-m parabolic antennas. The dashed lines refer to using a 34-m parabolic antenna on the Earth. For $f > 60$ GHz, only 45° (with a 34-m antenna) and 90° slant paths are allowed.

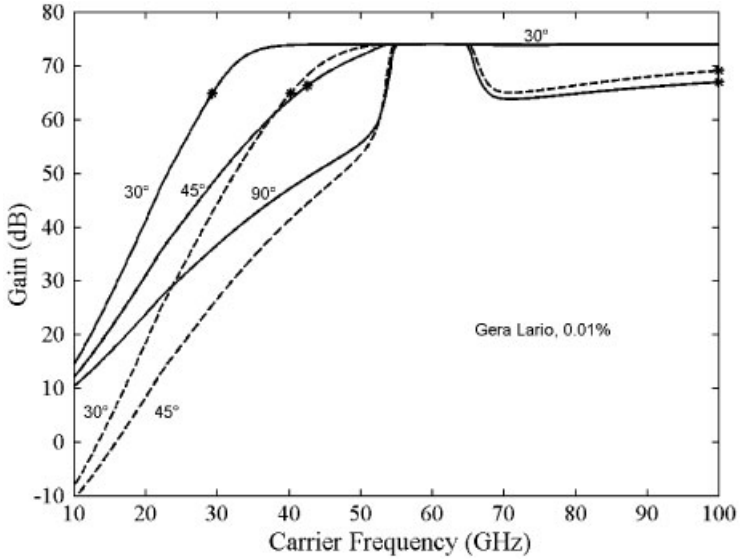

Figure 4. Gain (dB) as a function of carrier frequency ($f_2 = f_1$) and elevation angle. Mars–Earth downlink with a transparent transponder onboard a (geostationary) satellite, with $P_{t1} = P_{t2} = 35$ W, 4 identical 2.5-m parabolic antennas. Gera Lario, fraction of time 0.01%. The dashed lines refer to using a 34-m parabolic antenna on the Earth. Asterisks show frequencies $f_{m,t}$ of the minima of $P(e)$, in the frequency range 10–100 GHz. Beyond 60 GHz, the 30° continuous line refers also to 45°.

(and by Equation (20), for maximum capacity), for frequencies below 55 GHz if $\theta = 30^\circ$, and with values of $P(e)$ that are acceptable for a service from deep-space, i.e. $P(e) < 5 \times 10^{-3}$ for uncompressed photographs, or $P(e) < 10^{-7}$ for compressed photographs [13]. The minimum is beyond 65 GHz for $\theta = 90^\circ$ only. In this case, the proposal of using W-band (90 GHz) (e.g. Reference [11]), can be realistic and very useful, once efficient antennas and transmitters are fully developed for this frequency band. Notice that the use of a 34-m diameter receiving parabola on the Earth (dashed line) makes the 30° slant path performance equal to the 45° slant path performance obtained with the smaller antenna.

Figure 4 shows the gain of the 2-hop downlink, Equation (11). The gain is positive (in dBs) and very large, except for $f < 10$ GHz (e.g. for X-band). Using a 34-m parabolic antenna on the Earth makes $G < 0$ dB, i.e. the 1-hop downlink performs better, for $f < 15$ GHz (see Table I for the limit at low frequencies). In the range 55–65 GHz, even if $G \gg 0$ dB (the asymptote predicted by Equation (12)), the values of $P(e)$ obtainable are never acceptable ('forbidden' window). If we use a 1-hop downlink at a carrier frequency $f = f_{m,t}$, we need to gain many decibels in one of the parameters of Equation (9), e.g. power or effective area of the antennas, to compete with the 2-hop downlink. This makes the 1-hop downlink impossible to be implemented with the current technology.

Figure 5 shows the values of $1/R_{o,2h}$, i.e. the signal-to-noise power ratio corresponding to Figure 3. The maxima found here correspond, of course, to the minima of Figure 3.

Figure 6 shows how $R_{o,1}$ and $R_{o,2}$ add (in natural units according to (2)) and establish which hop determines the noise-to-signal ratio at the Earth receiving terminal. In this case $f_{m,t} = 42.6$ GHz, $f_e = 48.5$ GHz $> f_{m,t}$ as anticipated in Section 3, and $d_e \cong 0.5 d_1$ according to (8).

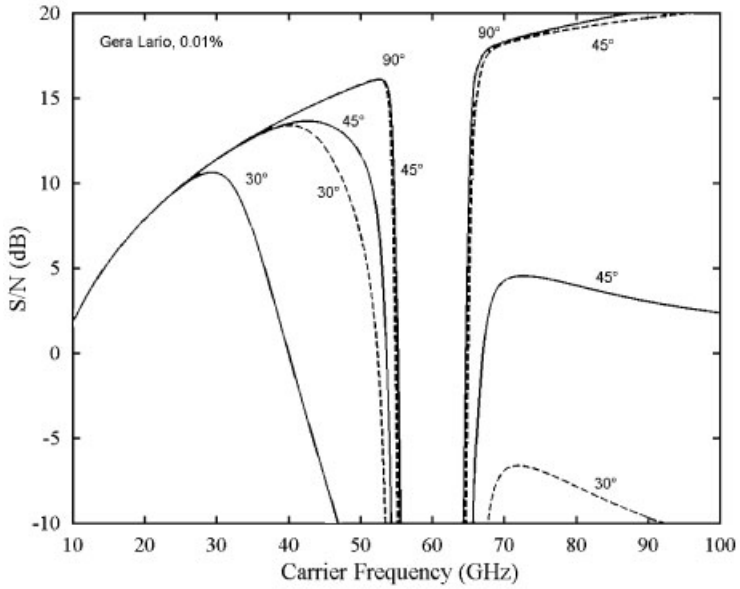

Figure 5. Values $1/R_{o,2h}$ (signal-to-noise power ratio) of a 2-hop downlink, with a transparent transponder onboard a (geostationary) satellite, as a function of carrier frequency ($f_2 = f_1$) and elevation angle, in the frequency range 10–100 GHz. Gera Lario, fraction of time 0.01%. Mars–Earth downlink, with $P_{t1} = P_{t2} = 35$ W, 4 identical 2.5-m parabolic antennas. The dashed lines refer to using a 34-m parabolic antenna on the Earth.

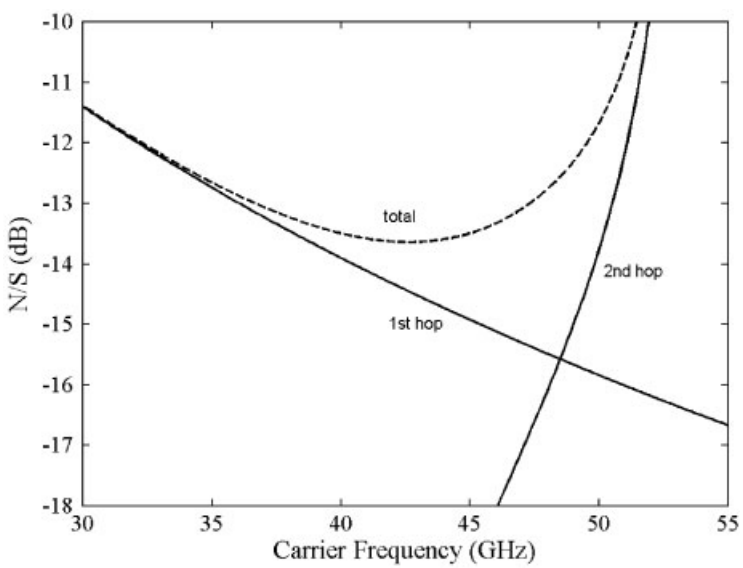

Figure 6. How with a transparent transponder $R_{o,1}$ (first hop) and $R_{o,2}$ (second hop), continuous lines, add (in natural units) to establish the total noise-to-signal ratio on the Earth, dashed line, as a function of carrier frequencies ($f_2 = f_1$), for $\theta = 45^\circ$ (see Figure 3). In this case $f_{m,t} = 42.6$ GHz, $f_e = 48.5$ GHz (crossing of the two continuous lines).

Figures 7 and 8 show the values of $P(e)$ and spacecraft and satellite transmitters' power as a function of $f_{m,t}$ and elevation angle, for 2.5 m diameter antennas. Notice again the impact of using a 34-m antenna on the Earth.

Let us now consider a *regenerative* transponder. The sensitivity to changes in the power transmitted by the satellite can be assessed in Figure 9. As anticipated, the minima, at $f_{m,r}$, are

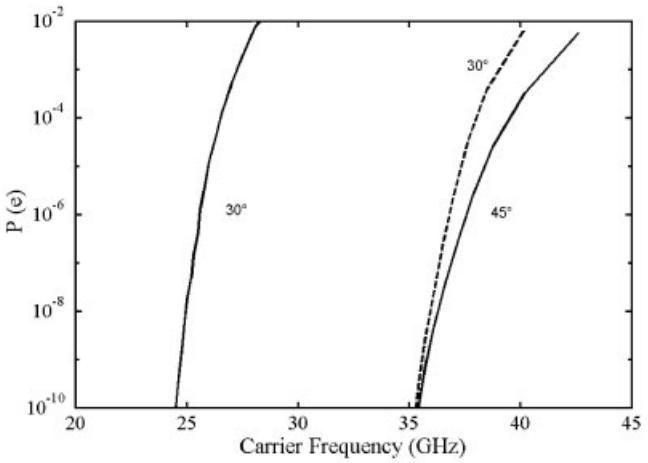

Figure 7. Probability of bit error as a function of $f_{m,t}$ ($f_2 = f_1$) and elevation angle 30° and 45°. Mars–Earth downlink with a transparent transponder onboard a (geostationary) satellite, with $P_{t1} = P_{t2} = 35$ W, 4 identical 2.5-m parabolic antennas. The dashed lines refer to using a 34-m parabolic antenna on the Earth.

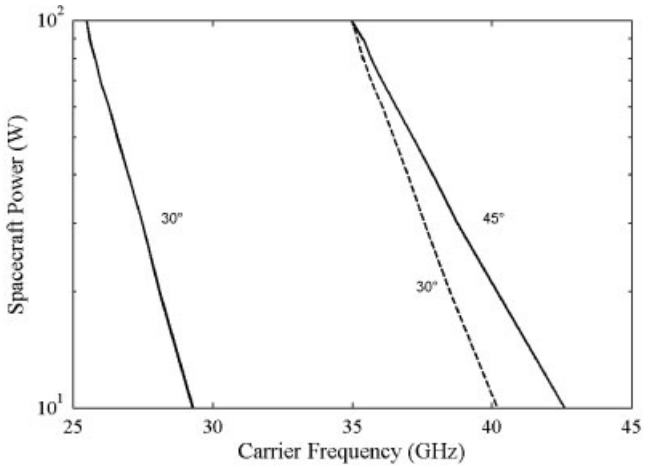

Figure 8. Spacecraft (and satellite power) as a function of $f_{m,t}$ ($f_2 = f_1$) and elevation angle 30° and 45°. Mars–Earth downlink with a transparent transponder, with $P_{t1} = P_{t2} = 35$ W, 4 identical 2.5-m parabolic antennas. Gera Lario, fraction of time 0.01%. The dashed lines refer to using a 34-m parabolic antenna on the Earth.

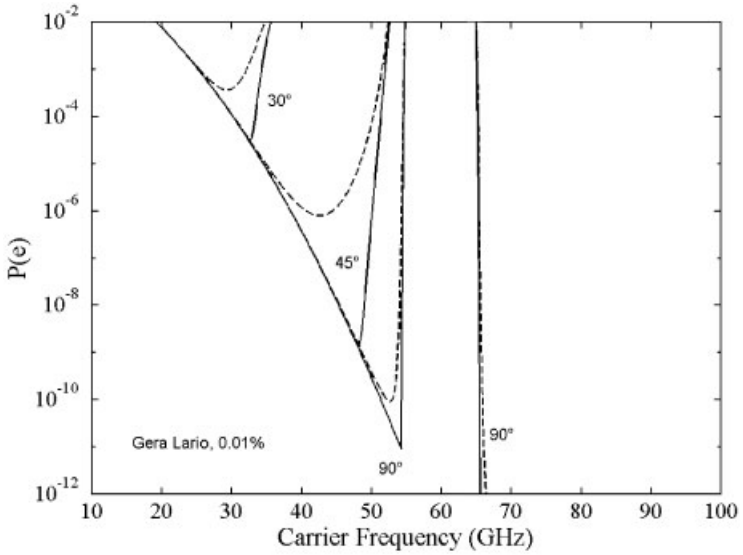

Figure 9. Probability of bit error as a function of carrier frequency ($f_2 = f_1$) and elevation angle. Mars–Earth downlink, with $P_{t1} = P_{t2} = 35$ W, 4 identical 2.5-m parabolic antennas. Gera Lario, fraction of time 0.01%. The dashed lines refer to a transparent transponder, the continuous lines to a regenerative transponder, both onboard a (geostationary) satellite. For $f > 60$ GHz, only 90° slant paths are allowed.

deeper for a regenerative transponder, but they shift to higher frequencies practically coincident with f_e, as Figure 10 shows it in detail.

If we use a *space station* instead of a geostationary satellite, the gain and improvement are much larger because the free-space distance of the 2nd hop is much shorter ($\sim$ 200 km).

Figure 11 shows the capacity obtainable according to Shannon. It is two or three times larger than the bit rate assumed in the QPSK or BPSK ideal channel, i.e. 100 kbit/s.

10.3. Saturn–Earth downlink

Let us now consider a downlink from the planet Saturn. We investigate, for brevity, only a design that adopts two largely different frequencies and a transparent transponder onboard a geostationary satellite. As discussed in Section 3.3, the lower frequency should be adopted in the second hop to experiment and match a smaller troposphere attenuation, the higher one should be adopted in the first long hop to take advantage of the higher gain of antennas of fixed size.

Figures 12 and 13 show the values obtainable of $P(e)$ and G in a 30°-slant path at Gera Lario and Fucino, as a function of the carrier frequency used in the satellite–Earth hop, i.e. $f = f_2$, by keeping $f_1 = 90$ GHz. G does not show a horizontal asymptote. We notice that the frequency interval below 55 GHz is now largely available at Fucino, and partially available at Gera Lario, with a large gain, given by Equation (11), compared to a 1-hop downlink working at the same carrier frequency indicated in the abscissa. The frequency interval beyond 65 GHz is available only at Fucino.

Notice that at $f = f_2 = 32$ GHz, the values obtainable of $P(e)$ can be very much below 10^{-7} for Fucino and also for Gera Lario (with $P_{t2} = 100$ W). A 1-hop downlink at 32 GHz, with $P_{t1} = 100$ W, would need to gain between about 50 and 80 dBs (see Figure 13) to guarantee the same $P(e)$ and link-availability.

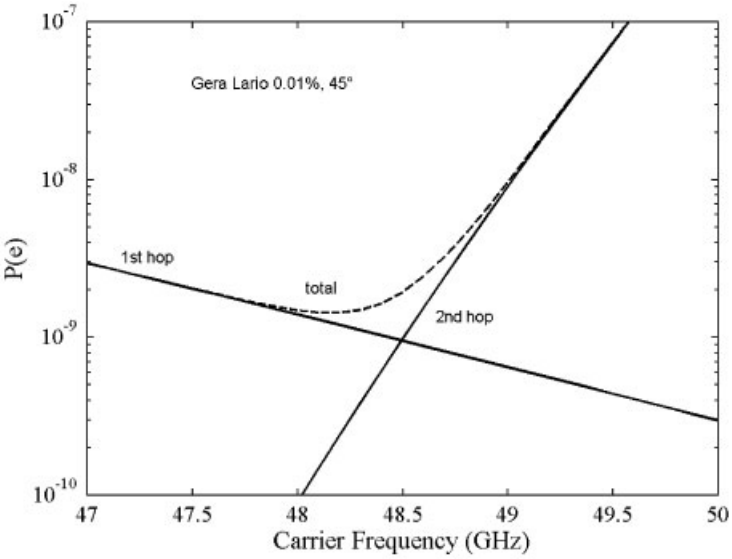

Figure 10. How with a regenerative transponder $P_1(e)$ (first hop) and $P_2(e)$ (second hop), continuous lines, add to establish the total probability of bit error on the Earth, dashed line, as a function of carrier frequencies ($f_2 = f_1$), for $\theta = 45^\circ$, $P_{t1} = P_{t2} = 35$ W, 4 identical 2.5-m parabolic antennas (see Figure 9). Gera Lario, fraction of time 0.01%. In this case $f_{m,r} = 48.2$ GHz, $f_e = 48.5$ GHz (crossing of the two continuous lines). Notice that for a regenerative transponder $f_{m,r} \approx f_e$.

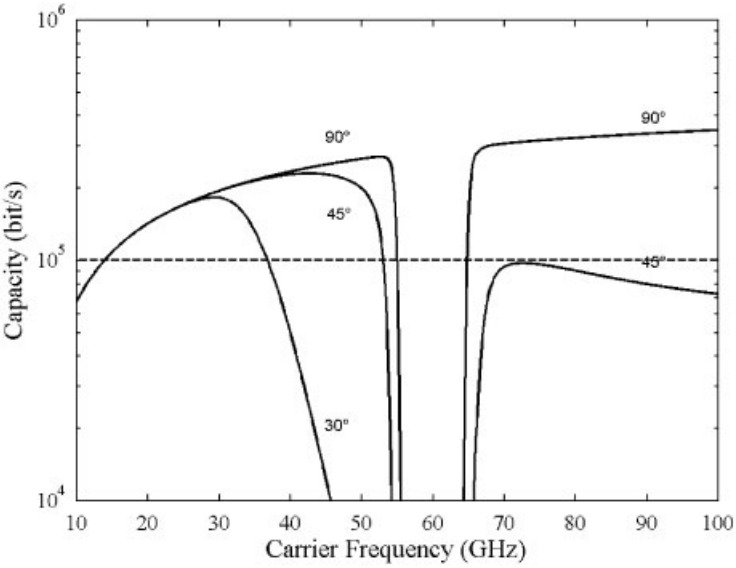

Figure 11. Shannon's capacity as a function of elevation angle. Gera Lario, fraction of time 0.01%, Mars–Earth downlink with a transparent transponder onboard a (geostationary) satellite, with $P_{t1} = P_{t2} = 35$ W, 4 identical 2.5-m parabolic antennas $B = B_e$ (roll-off factor equal to zero). The dashed lines refer to the BPSK or QPSK bit rate.

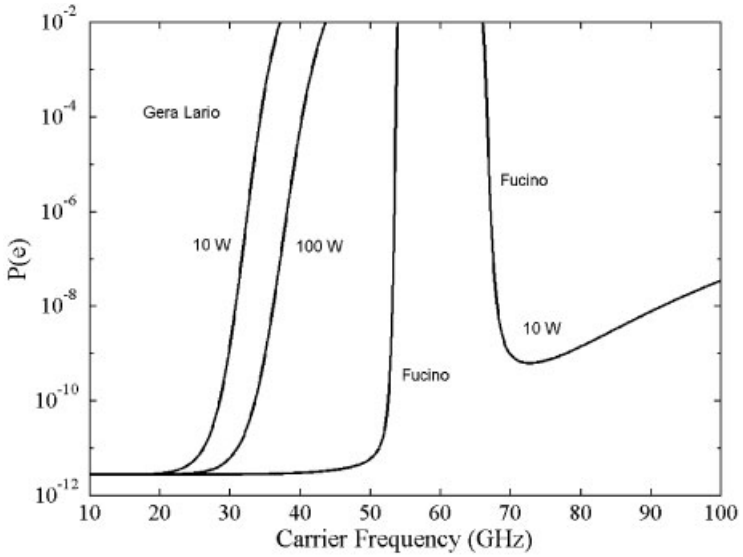

Figure 12. Probability of bit error in a 30°-slant path at Fucino and Gera Lario, in the Saturn–Earth downlink, as a function of the carrier frequency used in the satellite–Earth hop, f_2, in the frequency range 10–100 GHz. $P_{t2} = 10$ W (Fucino, Gera Lario) or $P_{t2} = 100$ W (Gera Lario), $P_{t1} = 100$ W, $f_1 = 90$ GHz, with four identical 4-m diameter antennas, and a transparent transponder onboard a (geostationary) satellite.

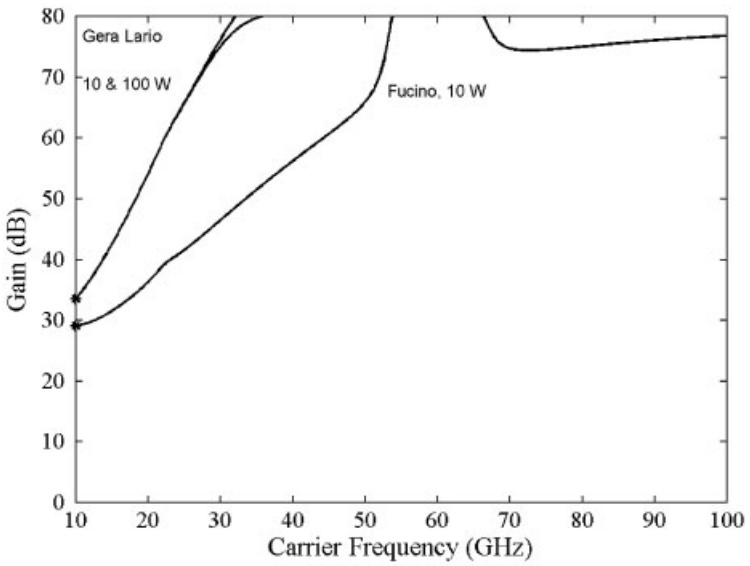

Figure 13. Gain (dB) in a 30°-slant path at Fucino and Gera Lario, in the Saturn–Earth downlink, as a function of the carrier frequency used in the satellite–Earth hop, f_2, in the frequency range 10–100 GHz. $P_{t2} = 10$ W (Fucino, Gera Lario) or $P_{t2} = 100$ W (Gera Lario), $P_{t1} = 100$ W, $f_1 = 90$ GHz, with four identical 4-m diameter antennas, and a transparent transponder onboard a (geostationary) satellite. Asterisks show frequencies of the (relative) minima of $P(e)$.

11. CONCLUSION

In our renewed study of a 2-hop downlink in deep-space communications in the frequency range 10–100 GHz, in which the first hop links the deep-space spacecraft (e.g. from Mars or Saturn) to a satellite orbiting around the Earth, and the second hop links the satellite to the final Earth terminal, we have shown that the performance of a 2-hop downlink can be superior to that of a 1-hop downlink, with a large gain G (or improvement I, figures of merit not independent) when high link-availability is required, i.e. when the attenuation of the Earth troposphere is large. The general findings and methodology are of global applicability. The 2-hop downlink can provide a communication capacity with high link-availability very difficult or impossible to achieve with a 1-hop downlink.

If we set $f_1 = f_2 = f$ in the two hops for BPSK or QPSK modulation schemes, and consider f a variable parameter, the noise-to-signal ratio, Equation (2) (transparent transponder), and the probability of bit error, Equation (13) (regenerative transponder), have a minimum value that, for a given site and attenuation considered (or corresponding fraction of time), can fall in a useful microwave range.

For BPSK or QPSK, a better choice is to assign a low carrier frequency to the second hop, to measure a smaller troposphere attenuation, and a high one to the first hop, to take advantage of the higher gain that antennas of fixed size can provide at very high microwave frequencies, such as W-band (90 GHz), as shown for the Saturn–Earth downlink, once the technology for this band is mature. In other words, by setting $f_2 \neq f_1$ with $f_2 \ll f_1$, each hop can be designed more independently for a high link-availability.

Table I has compared the design with $f_2 = f_1$ to the design with $f_2 \neq f_1$ for BPSK or QPSK. Table II has compared the two designs according to Shannon's capacity theorem. This latter table is fundamental because it provides the maximum power reduction G_p (or gain) theoretically obtainable in the 2-hop downlink, compared to the 1-hop downlink, for the same performance.

By a 2-hop downlink, the deep-space spacecraft would communicate as if it were transmitting 'from the Earth' through a conventional satellite connection, so that the Earth receiver could be placed anywhere and be of relatively small size. Moreover, the carrier frequencies of a 2-hop downlink need not be restricted to those assigned to deep-space communication by international regulations, because the received power on Earth can be of the same order of magnitude of the other Earth-based satellite links and thus undergo the same constraints. On the contrary, the very low power received in a 1-hop downlink requires reserved frequency bands to avoid any kind of interference. A 2-hop downlink can be much more robust to interference.

Future basic research and work are necessary in the area of system architecture (see Reference [3] for an account of the many variables to be considered, although in optical communication in their case) and on overall costs of the 2-hop downlink compared to a 1-hop downlink.

APPENDIX A: RAIN ATTENUATION VERSUS CARRIER FREQUENCY

Rain attenuation, A_R (dB), exceeded in an average year for a fraction of time $P(\%)$, at a carrier frequency f (GHz), in a slant path at a reference elevation angle θ_o can be written (see Reference [5]) as

$$A_R(f) = C_1 e^{\delta_1 f} + C_2 e^{\delta_2 f} - (C_1 + C_2) \quad \text{(dB)} \tag{A1}$$

where the four constants C_1, C_2, δ_1, δ_2 are a function of P. For $P = 0.01\%$ considered in the paper, these constants, are given by $C_1 = -369.2$, $C_2 = 256.0$, $\delta_1 = -0.0503$, $\delta_2 = -0.0778$ for Gera Lario ($\theta_o = 33^\circ$), and $C_1 = -220.7$, $C_2 = 151.5$, $\delta_1 = -0.0420$, $\delta_2 = -0.0649$ for Fucino ($\theta_o = 32^\circ$).

Equation (A1) can be scaled to other elevation angles $\theta > 10^\circ$, according to the secant-law

$$A(\theta) = A(\theta_o)\sin\theta_o/\sin\theta \quad \text{(dB)} \tag{A2}$$

APPENDIX B: FREQUENCIES OF MINIMUM NOISE-TO-SIGNAL RATIO AND MAXIMUM CAPACITY

Let us first consider a transparent transponder with $f_2 = f_1 = f$ and consider f as a variable. Equation (2) can be written, for a given slant path with elevation angle θ, as

$$R_{o,2h}(f) = y(f) = a\left(\frac{d_1}{f}\right)^2 + b\left(\frac{d_2}{f}\right)^2 e^{2\alpha(f)} \tag{B1a}$$

in which

$$a = \frac{N_{o1}B_e c^2}{P_{t1}A_{t1}A_{r1}g_c} \tag{B1b}$$

$$b = \frac{N_{o2}B_e c^2}{P_{t2}A_{t2}A_{r2}g_c} \tag{B1c}$$

$$e^{2\alpha(f)} = 10^{A(f)/10} \tag{B1d}$$

The frequency derivative of (B1a) set to zero yields

$$a\frac{d_1^2}{f^3} + b\frac{d_2^2}{f^3}e^{2\alpha(f)} - b\frac{d_2^2}{f^2}e^{2\alpha(f)}\alpha'(f) = 0 \tag{B2}$$

in which $\alpha'(f)$ is the frequency derivative of the total attenuation $\alpha(f)$ expressed in Nepers. Since $f \neq 0$, Equation (B2) can be written as

$$a\left(\frac{d_1}{f}\right)^2 + b\left(\frac{d_2}{f}\right)^2 e^{2\alpha(f)} = b\frac{d_2^2}{f}e^{2\alpha(f)}\alpha'(f) \tag{B3}$$

that, by recalling (B1a) can be written as

$$\begin{aligned} R_{o,2h}(f_{m,t}) &= b\frac{d_2^2}{f_{m,t}}e^{2\alpha(f)}\alpha'(f_{m,t}) \\ &= \frac{N_{o2}B_e c^2}{P_{t2}A_{t2}A_{r2}g_c} \times \frac{d_2^2 \times 10^{A(f)/10}}{f_{m,t}}\alpha'(f) \\ &= \frac{N_{o2}B_e c^2}{P_{t2}A_{t2}A_{r2}g_c} \times \frac{d_e^2}{f_{m,t}}\alpha'(f_{m,t}) \end{aligned} \tag{B4}$$

Notice that, once $R_{o,2h}(f_{m,t})$ is fixed, the frequency of minimum, $f_{m,t}$, is a function only of the second hop. Equation (B4) gives also the frequencies of maximum capacity (see Section 8).

Let us consider now a regenerative transponder. We should consider Equation (14) and its frequency derivative set to zero. The calculations are straight but lengthy. However, as we have shown graphically (see Figure 10), we can assume, for the minima of the probability of bit error, that $f_{\mathrm{m,r}} \approx f_{\mathrm{e}}$, the latter given by Equation (5).

Equation (1) is a very good approximation of a 2-hop downlink noise-to-signal ratio. If P_{t2} is the total power transmitted by the satellite, a small fraction of it will be used to transmit the amplified noise of the first hop. This power is given by

$$P_{t2}^{(n)} = P_{t2}\frac{N_{o1}B_e}{N_{o1}B_e + P_{r1}} \tag{B5}$$

The power transmitted for the signal is

$$P_{t2}^{(s)} = P_{t2}\frac{P_{r1}}{N_{o1}B_e + P_{r1}} \tag{B6}$$

Now the total noise power density at the Earth receiver is then given by

$$N_o = P_{r2}\frac{N_{o1}}{N_{o1}B_e + P_{r1}} + N_{o2} \tag{B7}$$

The 2-hop noise-to-signal ratio is then given by

$$R_{o,2h} = \frac{N_{o1}B_e}{P_{r1}} + \frac{N_{o2}B_e}{P_{r2}\dfrac{P_{r1}}{N_{o1}B_e + P_{r1}}} = R_{o,1} + R_{o,2}\frac{N_{o1}B_e + P_{r1}}{P_{r1}}$$

$$= R_{o,1} + R_{o,2}(1 + R_{o,1}) \approx R_{o,1} + R_{o,2} \tag{B8}$$

because in a real system, for an acceptable probability of bit error, $R_{o1} \ll 1$.

REFERENCES

1. Edwards CD, Stelzried CT, Deutsch LJ, Swanson L. NASA's deep-space telecommunications road map. *The Telecommunications and Mission Operations Progress Report*, Jet Propulsion Laboratory, 15 February, 1999; 42–136.
2. Gilchriest CE. Spacecraft mass trade-offs versus radio-frequency power and antenna size at 8 GHz and 32 GHz. *The Telecommunications and Data Acquisition Progress Report*, Jet Propulsion Laboratory, January–March 1987; 42–89.
3. Wilson KE, Wright M, Cesarone R, Ceniceros J, Shea K. Cost and performance of an earth-orbiting optical communication relay transceiver and a ground-base optical receiver subnet. *The Interplanetary Network Progress Report*, Jet Propulsion Laboratory, 15 May, 2003; 42–153.
4. Koerner MA. A bent pipe design for relaying signals received by an orbiting deep space relay station to a ground station. *The Deep Space Network Progress Report*, Jet Propulsion Laboratory, January–February 1980; 42–56, 76–84.
5. Matricciani E, Riva C. Evaluation of the feasibility of satellite systems design in the 10–100 GHz frequency range. *International Journal of Satellite Communications* 1998; **16**:237–247.
6. ITU-R. Propagation data and prediction methods required for the design of Earth-space telecommunication systems. *Rec. P.618-7*, 2001.
7. ITU-R. Attenuation by atmospheric gases. *Rec. P.676-5*, 2001.
8. ITU-R. Attenuation due to clouds and fog. *Rec. P.840-3*, 1999.
9. Panter PF. *Communication Systems Design: Line-of-sight and Tropo-scatter*. McGraw-Hill: New York, 1972.

10. Davarian F, Shambayati S, Slobin S. Deep space ka-band link management and Mars reconnaissance orbiter: long-term weather statistics versus forecasting. *Proceedings of the IEEE*, vol. 92. December 2004; 1879–1894.
11. Shambayati S. On the use of W-band for deep-space communications. *The Interplanetary Network Progress Report*, Jet Propulsion Laboratory, 15 August, 2003; 42–155.
12. Williamson M. Deep space communications. *IEE Review* 1998; **44**:119–122.
13. Communicating across the solar system, editorial. *IEEE Aerospace Electronic Systems Magazine* (Jubilee Issue). October 2000; 108–117.
14. Pratt T, Bostian CW, Allnutt JE. *Satellite Communications* (2nd edn). Wiley: New York, 2003.
15. Haykin S. *Communication Systems* (4th edn). Wiley: New York, 2001.

AUTHOR'S BIOGRAPHY

Emilio Matricciani was born in Italy in 1952. After serving in the Army, he received the Laurea degree in Electronics Engineering from Politecnico di Milano, Milan, Italy, in 1978. He joined Politecnico di Milano in 1978 as a recipient of a research scholarship in Satellite Communications, and in 1981, he became an Assistant Professor of Electrical Communications. In 1987, he joined the Universitá di Padova, Padua, Italy, as an Associate Professor of Microwaves. Since 1991, he has been with Politecnico di Milano as an Associate Professor of Electrical Communications. In the year 2001, he qualified as a Full Professor of Telecommunications. He has been involved in the experiments conducted with the Italian satellite Sirio in the 1970s in the 12–14 and 18 GHz bands, and afterwards, in the planning and conducting the experiments with Italsat in the 20–30 and 40–50 GHz bands, in the 1980s and 1990s. His actual research interests include satellite communications for fixed and mobile systems, radio wave propagation, history of science and technology. He teaches the course of Communication Systems to undergraduate students and Engineering of Satellite Communication Systems to graduate students. In addition to these institutional activities, he also teaches the fundamental aspects of communicating scientific and technical information, to undergraduate, graduate, master and doctorate students.

